[Frontiers In Bioscience, Landmark, 22, 1644-1654, June 1, 2017]

FLAG-tagged CD19-specific CAR-T cells eliminate CD19-bearing solid tumor cells *in vitro* and *in vivo*

Robert Berahovich[1], Shirley Xu[1], Hua Zhou[1], Hizkia Harto[1], Qumiao Xu[1], Andres Garcia[1], Fenyong Liu[2], Vita Golubovskaya[1], Lijun Wu[1]

[1]ProMab Biotechnologies, Richmond, CA, [2]Department of Infectious Diseases, University of California, Berkeley, CA

TABLE OF CONTENTS

1. ABSTRACT

Autologous T cells expressing chimeric antigen receptors (CARs) specific for CD19 have demonstrated remarkable efficacy as therapeutics for B cell malignancies. In the present study, we generated FLAG-tagged CD19-specific CAR-T cells (CD19-FLAG) and compared them to their non-tagged counterparts for their effects on solid and hematological cancer cells *in vitro* and *in vivo*. For solid tumors, we used HeLa cervical carcinoma cells engineered to overexpress CD19 (HeLa-CD19), and for hematological cancer we used Raji Burkitt's lymphoma cells, which endogenously express CD19. Like non-tagged CD19 CAR-T cells, CD19-FLAG CAR-T cells expanded in culture >100-fold and exhibited potent cytolytic activity against both HeLa-CD19 and Raji cells *in vitro*. CD19-FLAG CAR-T cells also secreted significantly more IFN-gamma and IL-2 than the control T cells. *In vivo*, CD19-FLAG CAR-T cells significantly blocked the growth of HeLa-CD19 solid tumors, increased tumor cleaved caspase-3 levels, and expanded systemically. CD19-FLAG CAR-T cells also significantly reduced Raji tumor burden and extended mouse survival. These results demonstrate the strong efficacy of FLAG-tagged CD19 CAR-T cells in solid and hematological cancer models.

2. INTRODUCTION

Chimeric antigen receptor (CAR)-expressing T cells have demonstrated remarkable efficacy against

B cell malignancies, including acute lymphoblastic leukemia, chronic lymphocytic leukemia, diffuse large B cell lymphoma, follicular lymphoma and mantle cell lymphoma (1-4). The CARs contain an extracellular single-chain variable fragment (scFv) specific for human CD19, along with a hinge region, a transmembrane domain and intracellular activation and costimulation domains (5-7). In clinical trials, CD19 CAR-T cells have yielded response rates of 50-80% in refractory lymphomas and 80-90% in acute lymphoblastic leukemia (7).

To monitor the CAR-T cells in the patient, the CAR-T cells must be labeled in some way. One method is to couple CAR expression with the expression of a marker, such as the truncated extracellular domain of the epidermal growth factor receptor (tEGFR); this coupling can be achieved using a ribosome-skipping T2A peptide (8). Another method, used in universal CARs, is to incorporate a binding site for the peptide portion of a "switch" which determines the specificity of the CAR-T cells (9). Yet another method is to generate anti-idiotype antibodies (10) or soluble recombinant ligands which bind to the scFv (11), (12).

A more direct method for CAR-T cell tracking is to attach a tag, such as the FLAG epitope, directly to the CAR. However, investigators are concerned that (1) the tag might be immunogenic, causing the patient's immune system to attack the CAR-T cells, and (2) that the tag might impair the expression or activity of the CAR. In the case of the FLAG epitope, a recent study has shown that the tag is not immunogenic in primates (13). However, studies have not been performed to evaluate whether the FLAG tag affects CAR-T cell function.

In this study, we hypothesized that the addition of a FLAG tag to the CD19 CAR would not affect its function *in vitro* or *in vivo,* and therefore might be advantageous for clinical studies (for example, detection of CAR-T cells with an antibody specific for the FLAG tag). Therefore, we determined the effects of inserting the FLAG tag into a CD19-specific CAR on CAR expression, CAR-T cell expansion and CAR-T cell cytotoxicity *in vitro*. For the target cells, we used Raji, a B lymphoid cancer line endogenously expressing CD19, and the novel cell line HeLa-CD19 (HeLa cervical carcinoma cells stably overexpressing CD19). In addition, we analyzed the efficacy of CD19-FLAG CAR-T cells in xenograft mouse models with Raji or Hela-CD19 tumors. The data indicate that the FLAG tag does not impair CAR-T cell expansion or cytotoxicity *in vitro*, and that CD19-FLAG CAR-T cells exhibit significant anti-tumor activity *in vivo*. Although CD19-FLAG CAR-T cells secreted much IFN-γ and IL-2 in response to Raji and HeLa-CD19 cells, the amounts of each cytokine were lower than those produced by non-tagged CD19-CAR-T cells, suggesting a potential safety advantage for future clinical use. Thus, CD19-FLAG CAR-T cells can be used in future clinical studies.

3. MATERIALS and METHODS

3.1. Cell lines

HeLa cells were purchased from the ATCC (Manassas, VA) and cultured in DMEM (*GE Healthcare*, Chicago, IL) containing 10% FBS (*AmCell*, Mountain View, CA). Raji cells and K562 cells were purchased from the ATCC and cultured in RPMI-1640 medium (*Thermo Fisher*, Waltham, MA) containing 10% FBS. Human peripheral blood mononuclear cells (PBMC) were isolated by density sedimentation over Ficoll-Paque (*GE Healthcare*). HEK293FT cells were a gift from *AlStem* (Richmond, CA) and were cultured in DMEM containing 10% FBS. All cell lines were authenticated by flow cytometry in our laboratory, using cell-specific surface markers.

3.2. CAR constructs

The mouse FMC63 anti-CD19 scFv (3) was inserted into a second-generation CAR cassette containing a signaling peptide from GM-CSF, a hinge region, transmembrane domain and costimulatory domain from CD28, and the CD3ζ activation domain; this CAR is herein called the CD19 CAR. The FLAG tag (DYKDDDDK) was inserted into the CD19 CAR between the scFv and hinge region; this CAR is herein called the CD19-FLAG CAR. An scFv specific for an intracellular protein was used instead of the FMC63 scFv; this CAR is herein called the mock CAR.

3.3. Generation of CAR-encoding lentivirus

DNAs encoding the CARs were synthesized and subcloned into a third-generation lentiviral vector, Lenti CMV-MCS-EF1a-puro by Syno Biological (Beijing, China). All CAR lentiviral constructs were sequenced in both directions to confirm CAR sequence and used for lentivirus production. Ten million growth-arrested HEK293FT cells (*Thermo Fisher*) were seeded into T75 flasks and cultured overnight, then transfected with the pPACKH1 Lentivector Packaging mix (*System Biosciences*, Palo Alto, CA) and 10 μg of each lentiviral vector using the CalPhos Transfection Kit (*Takara*, Mountain View, CA). The next day the medium was replaced with fresh medium, and 48 h later the lentivirus-containing medium was collected. The medium was cleared of cell debris by centrifugation at 2100 *g* for 30 min. The virus particles were collected by centrifugation at 112,000 *g* for 100 min, suspended in AIM V-AlbuMAX medium (*Thermo Fisher*), aliquoted and frozen at -80 °C. The titers of the virus preparations were determined by quantitative RT-PCR using the Lenti-X qRT-PCR kit (*Takara*) and the 7900HT thermal cycler (*Thermo Fisher*). The lentiviral titers were >$1x10^8$ pfu/ml. Lentiviruses were generated and used in accordance with approved biosafety level-2 regulations.

3.4. Generation and expansion of CAR-T cells

PBMC were isolated from human peripheral blood buffy coats (provided by the Stanford University Blood Center in accordance with its approved IRB protocol) suspended at 1 x 10^6 cells/ml in AIM V medium containing 10% FBS and 300 U/ml IL-2 (*Thermo Fisher*), mixed with an equal number (1:1 ratio) of CD3/CD28 Dynabeads (*Thermo Fisher*), and cultured in non-treated 24-well plates (0.5 ml per well). At 24 and 48 hours, lentivirus was added to the cultures at a multiplicity of infection (MOI) of 5, along with 1 μl of TransPlus transduction enhancer (*AIStem*). As the T cells proliferated over the next two weeks, the cells were counted every 2-3 days and fresh medium with 300 U/ml IL-2 was added to the cultures to maintain the cell density at 1-3 x 10^6 cells/ml.

3.5. Flow cytometry

To measure CAR expression, 0.5 million cells were suspended in 100 μl of buffer (PBS containing 0.5% BSA) and incubated on ice with 1 μl of human serum (*Jackson Immunoresearch*, West Grove, PA) for 10 min. Then 1 μl of allophycocyanin (APC)-labeled anti-CD3 (*eBioscience*, San Diego, CA), 2 μl of 7-aminoactinomycin D (7-AAD, *BioLegend*, San Diego, CA), and 2 μl of either phycoerythrin (PE)-labeled anti-FLAG or its isotype control PE rat IgG2a (both from *BioLegend*) was added, and the cells were incubated on ice for 30 min. The cells were rinsed with 3 ml of buffer, then suspended in buffer and acquired on a FACSCalibur *(BD Biosciences*). Cells were analyzed first for light scatter versus 7-AAD staining, then the 7-AAD$^-$ live gated cells were plotted for CD3 staining versus FLAG staining or isotype control staining. For the mouse tumor studies, 100 μl of blood was stained at room temperature for 30 min with 1 μl of APC anti-CD3, 2 μl of fluorescein isothiocyanate (FITC)-labeled anti-CD8a (*eBioscience*), 2 μl of 7-AAD, and 2 μl of either PE anti-FLAG or PE rat IgG2a. Erythrocytes were lysed with 3.5 ml of RBC lysing solution (150 mM NH_4Cl, 10 mM $NaHCO_3$, 1 mM EDTA pH 8), then leukocytes were collected by centrifugation and rinsed with 2 ml of cold buffer before acquisition.

3.6. Generation of the stable HeLa-CD19 cell line

To generate HeLa cells stably expressing human CD19, a DNA encoding the human CD19 open reading frame was synthesized and subcloned into the pCD510 lentiviral vector (*System Biosciences*) by Syno Biological. Lentivirus containing the vector was made as described above. HeLa cells were infected with the lentivirus at an MOI of 5 and cultured in the presence of 1 μg/ml puromycin to generate resistant cells, herein called HeLa-CD19. The expression of CD19 was confirmed by flow cytometry with a CD19 antibody (*BioLegend*).

3.7. Real-time cytotoxicity assay (RTCA)

Adherent target cells (HeLa or HeLa-CD19) were seeded into 96-well E-plates (*Acea Biosciences,* San Diego, CA) at 1 x 10^4 cells per well and monitored in culture overnight with the impedance-based real-time cell analysis (RTCA) xCELLigence system (*Acea Biosciences*). The next day, the medium was removed and replaced with AIM V-AlbuMAX medium containing 10% FBS ± 1 x 10^5 effector cells (CAR-T cells or non-transduced T cells), in triplicate. The cells in the E-plates were monitored for another 2-3 days with the RTCA system, and impedance was plotted over time. Cytolysis was calculated as (impedance of target cells without effector cells – impedance of target cells with effector cells) x100 / impedance of target cells without effector cells. For non-adherent target cells (Raji), the E-plates were first coated with an anti-CD40 antibody *(Acea Biosciences*). Then 1 x 10^4 Raji cells were plated per well and the RTCA assay was performed as described above.

3.8. Cytokine induction assay

The target cells (Raji, K562, HeLa or HeLa-CD19) were cultured with the effector cells (CAR-T cells or non-transduced T cells) at a 1:1 ratio (1 x 10^4 cells each) in U-bottom 96-well plates with 200 μl of AIM V-AlbuMAX medium containing 10% FBS, in triplicate. After 16 h the top 150 μl of medium was transferred to V-bottom 96-well plates and centrifuged at 300 g for 5 min to pellet any residual cells. The top 120 μl of supernatant was transferred to a new 96-well plate and analyzed by ELISA for human IFN-γ and IL-2 levels using kits from *Thermo Fisher* according to the manufacturer's protocol.

3.9. Mouse tumor studies

Six-week old male NSG mice (*Jackson Laboratories*, Bar Harbor, ME) were housed and manipulated in strict accordance with the Institutional Animal Care and Use Committee (IACUC). Each mouse was injected subcutaneously on day 0 with 100 μl of sterile PBS containing 2 x 10^6 HeLa-CD19 cells. In one study, CAR-T cells in PBS were injected intra-tumorally on days 19 (5 x 10^6 cells) and 33 (9 x 10^6 cells), and tumor growth was analyzed. In another study, CAR-T cells were injected intravenously on days 8 and 14 (1 x 10^7 cells each day). Tumor sizes were measured with calipers twice-weekly and tumor volume (in mm^3) was determined using the formula $W^2L/2$, where W is tumor width and L is tumor length. Tumors were excised and fixed in 4% paraformaldehyde, then embedded in paraffin wax and stained by immunohistochemistry. At the end of the intravenous CAR-T cell study, 100 μl of blood was collected and stained with different antibodies by flow cytometry as indicated above. For the Raji tumor

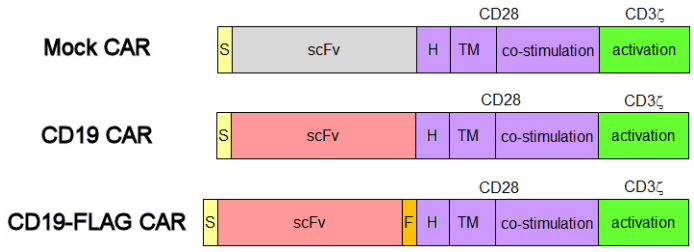

Figure 1. Schematic of the CAR constructs in this study. Abbreviations: S, signal peptide from GM-CSF; H, hinge region from CD28; TM, transmembrane domain from CD28; F, FLAG epitope.

model, mice were injected intravenously with 100 μl of sterile PBS containing 5 x 10^5 luciferase-expressing Raji cells, and the next day 5 x 10^6 CD19-FLAG CAR-T cells in 0.2 ml of PBS were injected intravenously. On days 6 and 14, the mice were imaged with the Xenogen IVIS Spectrum (*PerkinElmer*, Waltham, MA) system and tumor growth was monitored by measuring bioluminescence in photons per seconds.

3.10. Immunohistochemistry (IHC)

Tumor tissue sections (4 μm) were deparaffinized in xylenes twice for 10 min, then hydrated in graded alcohols and rinsed in PBS. Antigen retrieval was performed for 20 min in a pressure cooker using 10 mM citrate buffer, pH 6.0. The sections were cooled, rinsed with PBS, incubated in a 3% H_2O_2 solution for 10 min, and rinsed with PBS. The tissue sections were incubated in goat serum for 20 min and then incubated with rabbit anti-cleaved caspase-3 (Asp175, *Cell Signaling Technology*, Danvers, MA) or rabbit IgG (*Jackson Immunoresearch*) at 0.2 μg/ml overnight at 4 °C. The sections were rinsed with PBS, incubated with biotin-conjugated goat anti-rabbit IgG for 10 min, rinsed with PBS, incubated with streptavidin-conjugated peroxidase for 10 min, and rinsed with PBS. Finally, the sections were incubated in DAB substrate solution for 2-5 min, immersed in tap water, counterstained with hematoxylin, rinsed with water, and dehydrated in graded alcohols and xylenes. Coverslips were mounted with glycerin. All reagents except those noted were from *MaiXin.BIO* (Fuzhou, China). Images were acquired on a Motic DMB5-2231PL microscope with Images Plus 2.0. software (*Motic*, Xiamen, China). To quantitate cleaved caspase-3 staining, six random microscopic fields from each tumor were analyzed with ImageJ software (National Institutes of Health). Each image was split into an RGB stack, then the area of the blue stack above an arbitrary threshold (80) was measured.

3.11. Statistical analysis

Data were analyzed and plotted with Prism software (*GraphPad*, San Diego, CA). Comparisons between two groups were performed by unpaired Student's t test, and comparisons between three groups were performed by one-way ANOVA with Tukey's post-hoc test, except where noted.

4. RESULTS

4.1. CD19-FLAG CAR-T cells expand >100 fold *in vitro*

A human CD19-specific CAR was constructed consisting of the FMC63 murine scFv; hinge, transmembrane and costimulation domains from human CD28; and the activation domain of human CD3ζ (Figure 1). A "mock" CAR with an scFv specific for an intracellular protein – and thus not reactive with intact cells – was constructed in the same manner (Figure 1). In addition, the 8-amino acid FLAG epitope was inserted between the scFv and hinge region of the CD19-specific CAR. Sequences for each CAR were transferred into a lentiviral vector downstream of the cytomegalovirus immediate-early promoter, and CAR-encoding lentivirus particles were produced by transient transfection of HEK293FT cells. The viruses were added at an MOI of 5 to activated human T cells, which were then cultured with IL-2 for 14 days. The CAR-T cells (mock, CD19, CD19-FLAG) expanded over 100-fold during this time (Figure 2), indicating that the FLAG tag did not impact CAR-T cell expansion. Analysis of the cells by flow cytometry indicated that the transduction efficiency was >70% (Figure 3). Thus, CD19-FLAG CAR-T expanded *in vitro* similarly to CD19-CAR-T cells.

4.2. CD19-FLAG CAR-T cells exhibit strong CD19-dependent cytolytic activity

The ability of the CD19 and CD19-FLAG CAR-T cells to kill CD19-bearing target cells was tested using two human cell lines: the B cell line Raji, which endogenously expresses CD19, and the cervical carcinoma line HeLa which was engineered to overexpress CD19. Cytolysis was detected using the real-time cell analysis (RTCA) xCELLigence system, which measures the impedance of the target cell monolayer over time; as the target cells are killed by the effector cells, the impedance of the monolayer

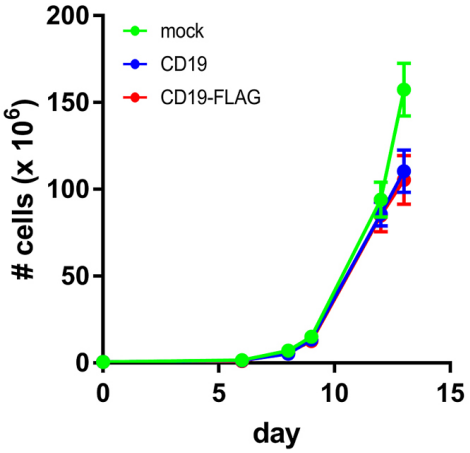

Figure 2. CD19-FLAG CAR-T cells exhibit comparable expansion to CD19 CAR-T cells. Mock CAR-T cells, CD19 CAR-T cells and CD19-FLAG CAR-T cells expanded >100-fold *in vitro*. A representative growth curve from three independent experiments is shown.

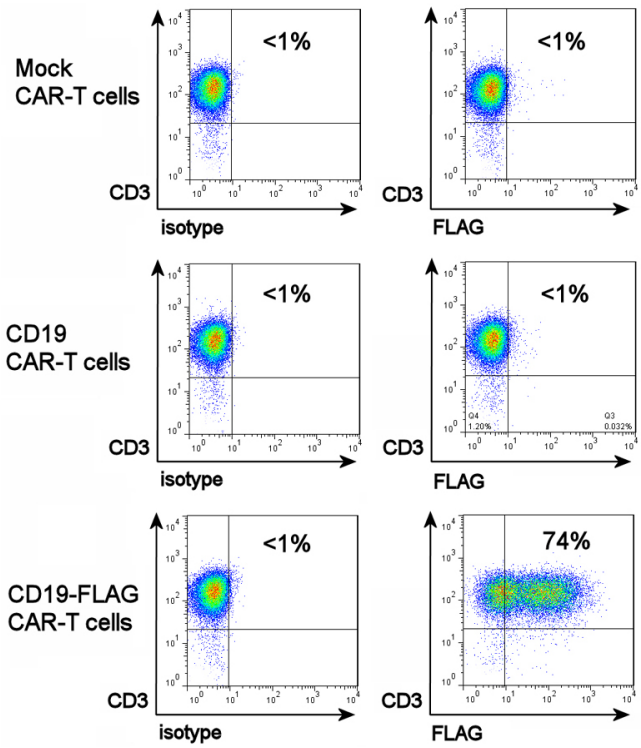

Figure 3. CD19-FLAG CAR-T cells exhibit high transduction efficiency. Mock CAR-T cells, CD19 CAR-T cells and CD19-FLAG CAR-T cells were stained by flow cytometry on day 8 of culture using an antibody against CD3 (Y-axis) and an antibody specific for the FLAG epitope (X-axis, right column) or its isotype control antibody (X-axis, left column).

decreases. The CD19 and CD19-FLAG CAR-T cells exhibited significant cytolytic activity against both Raji cells (Figure 4A) and Hela-CD19 cells (Figure 4B), but not against $CD19^-$ HeLa cells (Figure 4C). In contrast, mock CAR-T cells and non-transduced T cells did not exhibit significant cytolytic activity against any of the target cells. Thus, both CD19 and CD19-FLAG CAR-T cells exhibited strong CD19-dependent cytolytic activity.

4.3. CD19-FLAG CAR-T cells secrete IFN-γ and IL-2 in response to $CD19^+$ but not $CD19^-$ tumor cells

The CAR-T cells were evaluated for their ability to produce IFN-γ and IL-2 in response to $CD19^+$ target cells. Both CD19 and CD19-FLAG CAR-T cells produced significantly higher levels of IFN-γ (Figure 5 A-B) and IL-2 (Figure 5 C-D) when cultured with

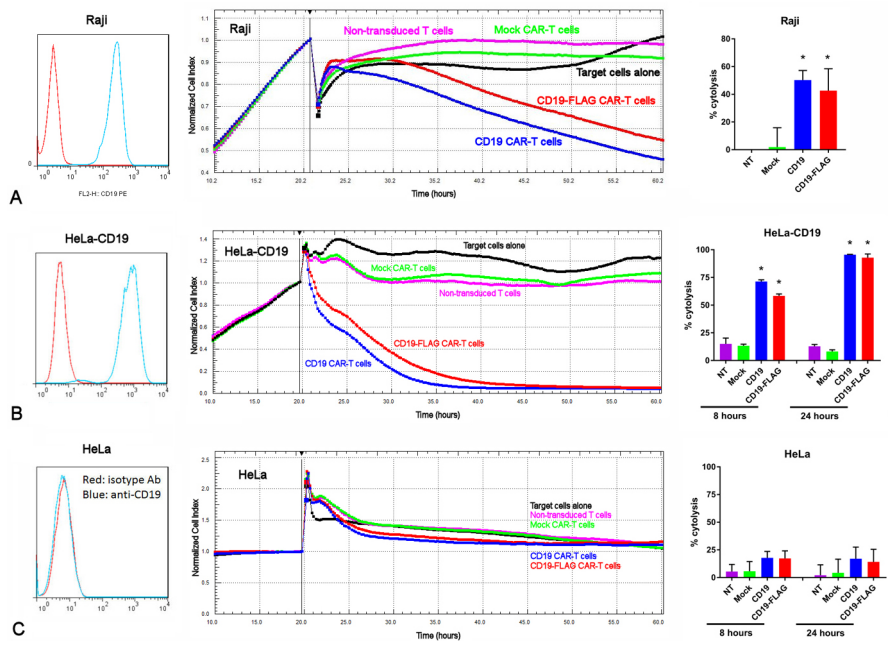

Figure 4. CD19-FLAG CAR-T cells are highly cytolytic for CD19⁺ cancer cells. A: Raji cells. Left: Flow cytometric staining with an antibody against CD19 (blue histogram) and an isotype control antibody (red histogram). Middle: the impedance of the tethered Raji cell monolayer is shown over time, with addition of non-transduced T cells, mock CAR-T cells, CD19 CAR-T cells or CD19-FLAG CAR-T cells at the vertical bar. Right: quantitation of cytolysis 40 hours after T cell addition; *: p<0.0.5 for CD19 or CD19-FLAG CAR-T cells compared to non-transduced T cells (NT) and to mock CAR-T cells. B: HeLa-CD19 cells. Left, middle and right: same as in panel A, with quantitation of cytolysis 8 and 24 hours after T cell addition; *: p<0.0.001 for CD19 or CD19-FLAG CAR-T cells compared to non-transduced T cells (NT) and to mock CAR-T cells. C: HeLa cells. Left, middle and right: same as in panel B. All conditions were performed in triplicate.

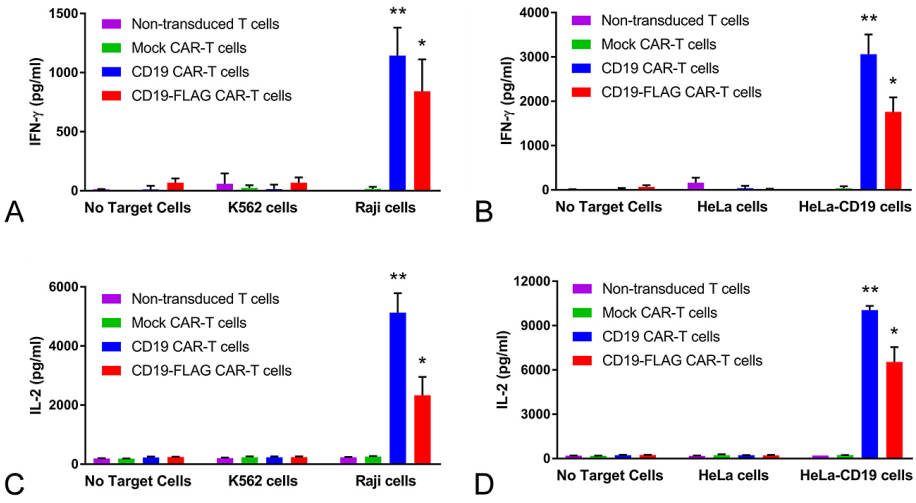

Figure 5. CD19-FLAG CAR-T cells produce moderate levels of IFN-γ and IL-2 in response to CD19⁺ cancer cells. A: IFN-γ production by non-transfected T cells, mock CAR-T cells, CD19 CAR-T cells or CD19-FLAG CAR-T cells after culture with endogenous CD19⁺ Raji cells or CD19⁻ K562 cells; **p=0.002 (CD19 CAR-T), *p=0.008 (CD19-FLAG CAR-T) for Raji cells over K562 cells. B: IFN-γ production by the same cell preparations after culture with CD19-overexpressing HeLa-CD19 cells or CD19⁻ HeLa cells; **p<0.0001 (CD19 CAR-T), *p=0.0003 (CD19-FLAG CAR-T) for HeLa-CD19 cells over HeLa cells. C: IL-2 production by the cell preparations after culture with endogenous CD19⁺ Raji cells or CD19⁻ K562 cells; **p<0.0001 (CD19 CAR-T), *p=0.002 (CD19-FLAG CAR-T) for Raji cells over K562 cells. D: IL-2 production by the cell preparations after culture with CD19-overexpressing HeLa-CD19 cells or CD19⁻ HeLa cells. **p<0.0001 (CD19 CAR-T), *p<0.0001 (CD19-FLAG CAR-T) for HeLa-CD19 cells over HeLa cells. All conditions were performed in triplicate.

CD19⁺ target cells (Raji and HeLa-CD19) than when cultured with CD19⁻ target cells (K562 and HeLa). Interestingly, the CD19-FLAG CAR-T cells produced lower levels of each cytokine than did the CD19 CAR-T cells. In contrast, the mock CAR-T cells and non-transduced T cells did not produce significant levels of either cytokine when cultured with any of the target cell lines. Thus, both CD19 and CD19-FLAG CAR-T cells secreted IFN-γ and IL-2 in a CD19-dependent manner.

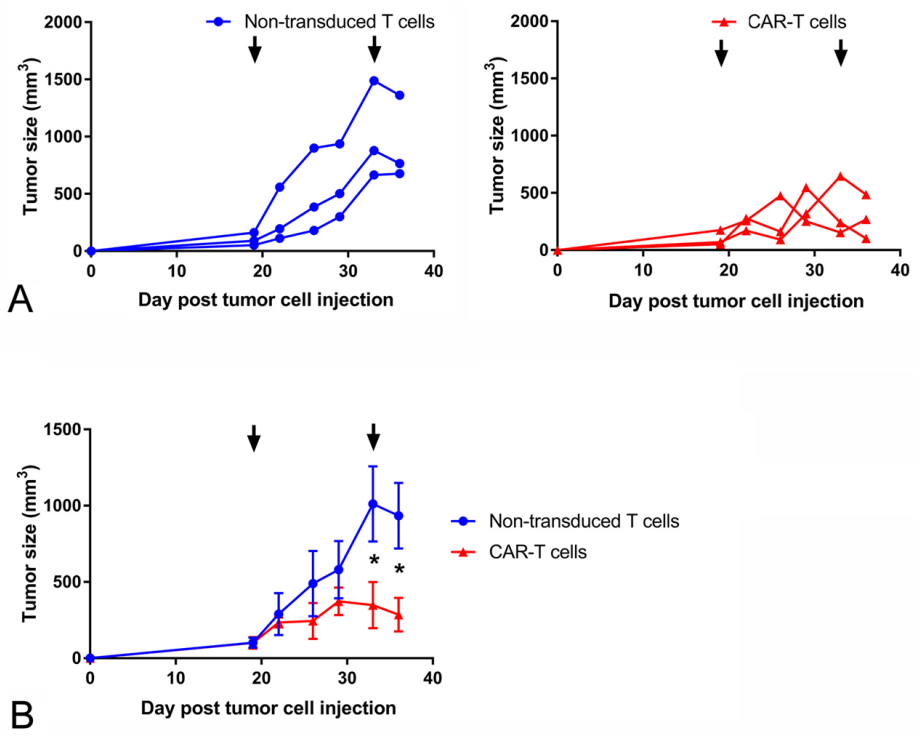

Figure 6. Intra-tumoral injections of CD19 and CD19-FLAG CAR-T cells significantly inhibit HeLa-CD19 tumor growth. A: growth curves for the tumors treated with non-transduced T cells (left) and the tumors treated with CD19 (day 19) and CD19-FLAG (day 33) CAR-T cells. B: tumor growth curves, averaged per group; *: $p<0.05$ for CAR-T cells compared to non-transduced T cells, determined by Student's t test assuming unequal variances.

4.4. CD19-FLAG CAR-T cells inhibit CD19$^+$ solid tumors *in vivo*

To determine the effect of CD19 and CD19-FLAG CAR-T cells on solid tumors *in vivo*, we developed a novel xenograft tumor model using the HeLa-CD19 cell line. Immunodeficient NSG mice were injected subcutaneously on each flank with 2 x 10^6 HeLa-CD19 cells, and the sizes of the tumors were monitored for 36 days. As shown in Figure 6, the tumors injected with CD19 and CD19-FLAG CAR-T cells (average 285 mm^3) were significantly smaller than the control tumors injected with non-transduced T cells (average 935 mm^3).

To characterize the effect of CD19-FLAG CAR-T cells in the HeLa-CD19 solid tumor model, a second study was conducted with earlier, intravenous application of the CD19-FLAG CAR-T cells. In this study, the CD19-FLAG CAR-T cells almost completely blocked tumor growth (Figure 7A-D), with no effect on mouse weight (Figure 7E). In addition, immunohistochemical analysis of the CD19-FLAG group tumor demonstrated an increased amount of cleaved caspase-3 compared to tumors from the two control groups (Figure 7F), indicating induced apoptosis of the tumor cells. Moreover, at the end of the study, the frequency of human T cells in the peripheral blood was 32.8 ± 4.9% in the CD19-FLAG group but only 3.8 ± 1.2% in the non-transduced T cell group (Figure 8A-B). Of the human T cells, the ratio of CD8$^+$ cells to CD8$^-$ cells was also higher in the CD19-FLAG group than the non-transduced T cell group (Figure 8C). Thus, CD19-FLAG CAR-T cells not only significantly blocked solid tumor growth but also systemically expanded *in vivo*.

4.5. CD19-FLAG CAR-T cells inhibit CD19+ hematological cancer *in vivo*

To analyze the effect of CD19-FLAG CAR-T cells on a hematological cancer *in vivo*, we injected NSG mice with luciferase$^+$ Raji cells and used IVIS *in vivo* imaging. Compared to the PBS control, CD19-FLAG cells significantly decreased Raji tumor cell burden (Figure 9 A-B) and significantly prolonged mouse survival (Figure 9C). The improved survival was similar to that seen previously with CD19 CAR-T cells (not shown).

5. DISCUSSION

In this study, we found that FLAG-tagged CD19-specific CAR-T cells are highly effective *in vitro* and *in vivo*. *In vitro*, CD19-FLAG CAR-T cells expanded over 100-fold, had a >70% transduction efficiency and were highly cytotoxic against CD19$^+$ but not CD19$^-$ cells. In addition, CD19-FLAG CAR-T cells were more effectively detected with an anti-FLAG antibody compared to CD19 CAR-T cells with an anti-mouse IgG F(ab')2 antibody (not shown),

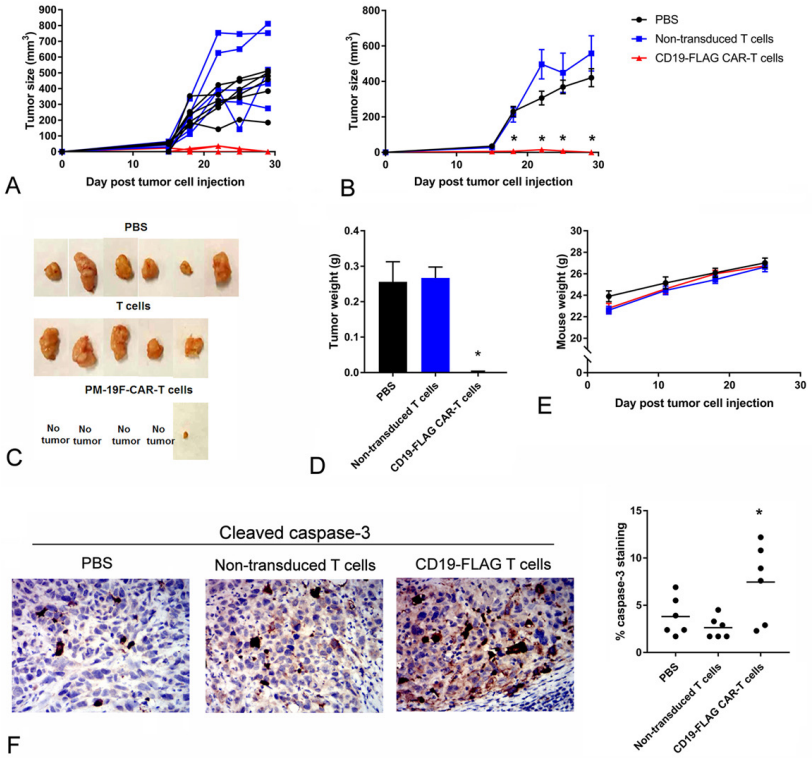

Figure 7. Intravenous injections of CD19-FLAG CAR-T cells significantly inhibit HeLa-CD19 tumor growth. A: Individual growth curves for the Hela-CD19 xenograft tumors. B: Hela-CD19 xenograft tumor growth curves, averaged per group; *: p<0.005 for CD19-FLAG CAR-T cells compared to non-transduced T cells. C: photographs of the tumors after dissection on day 29. D: average weights of the dissected xenograft tumors; *: p=0.002 CD19-FLAG CAR-T cells compared to non-transduced T cells. E: average body weights over the course of the study. F: Cleaved caspase-3 immunohistochemical staining (brown color): representative images (blue color = nucleus counterstain) and quantitation (six regions of each tumor); *: p=0.02 for CD19-FLAG CAR-T cells compared to non-transduced T cells.

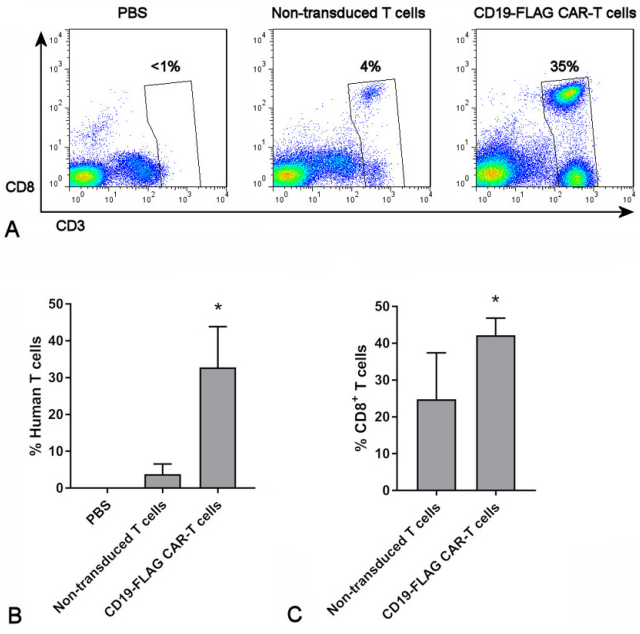

Figure 8. HeLa-CD19 tumor-bearing mice treated with CD19-FLAG CAR-T cells contain increased numbers of human T cells in the peripheral blood. A: representative human CD3 vs human CD8 flow cytometry plots from each group. Note the increased number of $CD8^+$ and $CD8^-$ cells in the drawn $CD3^+$ T cell gate in the CD19-FLAG plot. B: average frequency of human T cells among the peripheral blood leukocytes; *: p<0.0001 for CD19-FLAG CAR-T cells compared to non-transduced T cells. C: average frequency of $CD8^+$ cells among the human T cells; *: p=0.02 for CD19-FLAG CAR-T cells compared to non-transduced T cells.

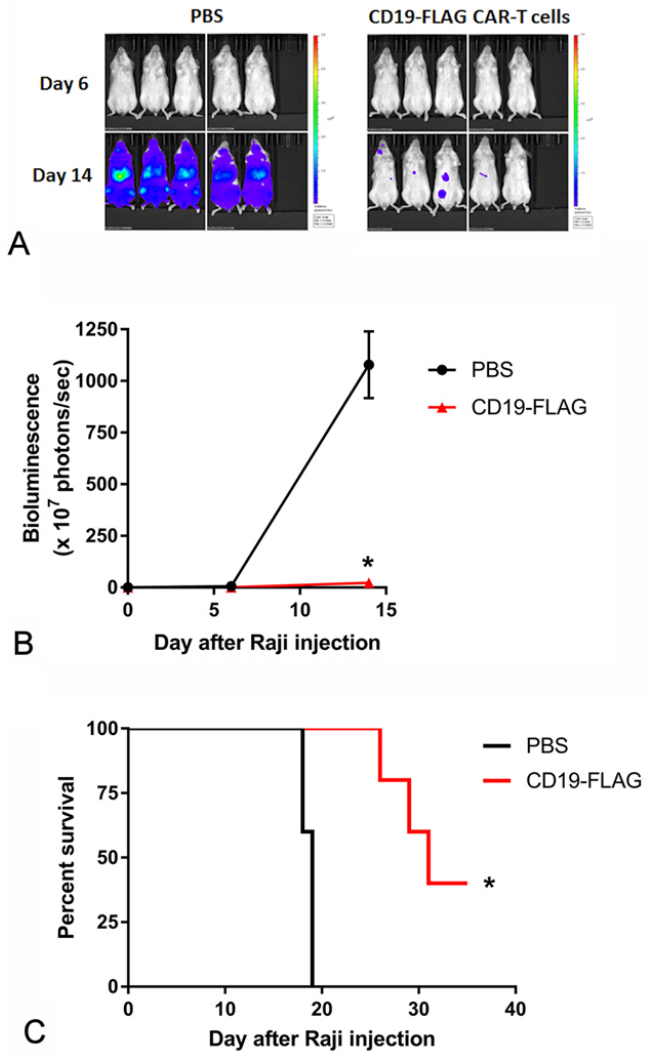

Figure 9. CD19-FLAG CAR-T cells significantly block Raji xenograft tumor growth and prolong survival. A: *in vivo* imaging of luciferase$^+$ Raji xenograft tumor cells in NSG mice. B: quantitation of the imaging data. Mice treated with CD19-FLAG CAR-T cells, but not PBS-treated mice, were almost completely free of Raji cells at day 14; *: p=0.0002. Error bars represent standard errors of the means. C: Kaplan-Meier survival plot showing that CD19-FLAG CAR-T cells significantly prolonged survival of mice in the Raji xenograft model; * p=0.003.

providing an advantage in CAR-T cell detection in future clinical studies. *In vivo*, CD19-FLAG CAR-T cells exhibited substantial anti-tumor activity against both CD19$^+$ solid tumors and CD19$^+$ hematological tumors. Efficacy *in vivo* was associated with CAR-T cell expansion, tumor cell apoptosis and increased animal survival.

We generated a novel solid tumor xenograft model using cervical cancer HeLa cells overexpressing CD19 in immunodeficient mice. This model allows us to study hematological cancer targets in the context of a solid tumor microenvironment and its associated inhibitory factors, such as immune checkpoint pathways (PD-1, CTLA-4, TIGIT, LAG-3), angiogenesis/vasculogenesis, and hypoxia. For example, PD-1 inhibition was recently shown to increase CAR-T cell efficacy (14),(15),(16). We found that CD19-FLAG CAR-T cells were highly efficient in blocking solid tumor growth despite these inhibitory factors. Similar models can be used for other hematological cancer antigens such as CD20, BCMA, CD22, CD38, CD138 and others. The model can also be used to study the microenvironment of hematological cancers (e.g. multiple myeloma) with bone marrow involvement. Targeting both tumor cells and the tumor microenvironment should provide a more effective anti-cancer therapy. Thus, our novel model can be used to probe the interactions of cancer cells with their microenvironment and potential therapeutics.

Although CD19-FLAG CAR-T cells were as cytotoxic as non-tagged CD19 CAR-T cells *in vitro*, CD19-FLAG CAR-T cells produced less IFN-γ and IL-2 than did the CD19 CAR-T cells. This result suggests that CD19-FLAG CAR-T cells might be less toxic than CD19 CAR-T cells *in vivo*, as high levels of cytokine secretion by CAR-T cells in patients often

lead to Cytokine Release Syndrome (CRS). In CRS, a systemic inflammatory response that can lead to death if untreated (17), (18), (19), (20), the patient experiences fever, hypotension, hypoxia, and neurologic disorders that may require aggressive medical support (20). The management and reversal of CRS includes high-dose steroids (>100 mg daily of prednisone) and the interleukin-6 receptor-blocking monoclonal antibody tocilizumab (20), (21). Recently, switch-off mechanisms such as the inducible caspase-9 suicide system were shown to block the activity and generation of CAR-T cells (22), (23). Hence, decreasing cytokine levels by using CD19-FLAG CAR-T cells instead of CD19 CAR-T cells might be advantageous in the clinic due to a decreased incidence of CRS. The decreased cytokine production of CD19-FLAG CAR-T cells might allow multiple applications, although this will require future clinical studies.

The use of CD19-FLAG CAR-T cells confers other benefits, as the FLAG tag can be used in the clinic for imaging the CAR-T cells after application, or beforehand for CAR-T cell sorting, manufacturing or other applications. Importantly, the FLAG tag is not immunogenic in primates (13), suggesting that it can be used for human studies. In that study, robust FLAG expression was detected for at least 5 months with no apparent immunogenicity (13).

FLAG-tagged CAR-T cells are not limited to hematological cancers, but can be used for solid cancers as well. In fact, we recently found that FLAG-tagged CAR-T cells specific for mesothelin were as effective as non-tagged mesothelin-specific CAR-T cells (not shown). As with CD19, mesothelin-FLAG CAR-T cells were better detected with the anti-FLAG antibody compared to mesothelin CAR-T cells with the anti-mouse IgG F(ab')2 antibody (not shown).

In sum, our study clearly demonstrates that CD19-FLAG CAR-T cells are highly efficacious and possess several advantages over non-tagged CD19 CAR-T cells that can be analyzed in future clinical studies.

6. ACKNOWLEDGMENTS

Robert Berahovich and Shirley Xu contributed equally to this article. We would like to thank Shuxiang Fu for help with the IHC staining, and Drs. Janet Yuejuan Li and Ed Lim for help with the mouse xenograft and imaging studies.

7. REFERENCES

1. Z Eshhar, G. Gross. Chimeric T cell receptor which incorporates the anti-tumour specificity of a monoclonal antibody with the cytolytic activity of T cells: a model system for immunotherapeutical approach. *Br J Cancer Suppl* 10, 27-29 (1990)

2. Z Eshhar, T Waks, T Gross. The emergence of T-bodies/CAR T cells. Cancer J *20*, 123-126 (2014)
DOI: 10.1097/PPO.0000000000000027

3. JN Kochenderfer, SA Feldman, Y Zhao, H Xu, MA Black, RA Morgan, WH Wilson, SA Rosenberg. Construction and preclinical evaluation of an anti-CD19 chimeric antigen receptor. *J Immunother* 32, 689-702 (2009)
DOI: 10.1097/CJI.0b013e3181ac6138

4. DL Porter, WT Hwang, NV Frey, SF Lacey, PA Shaw, AW Loren, A Bagg, KT Marcucci, A Shen, V Gonzalez, V. Chimeric antigen receptor T cells persist and induce sustained remissions in relapsed refractory chronic lymphocytic leukemia. *Sci Transl* Med *7*, 303ra139 (2015)
DOI: 10.1126/scitranslmed.aac5415

5. MV Maus, AR Haas, GL Beatty, SM Albelda, BL Levine, X Liu, Y Zhao, M Kalos, CH June. T cells expressing chimeric antigen receptors can cause anaphylaxis in humans. *Cancer Immunol Res 1*, 26-31 (2013)
DOI: 10.1158/2326-6066.CIR-13-0006

6. G Gross, T Waks, Z Eshhar. Expression of immunoglobulin-T-cell receptor chimeric molecules as functional receptors with antibody-type specificity. *Proc Natl Acad Sci U S A* 86, 10024-10028 (1989)
DOI: 10.1073/pnas.86.24.10024

7. A Fesnak, C Lin, DL Siegel, MV Maus. CAR-T Cell Therapies From the Transfusion Medicine Perspective. *Transfus Med Rev* 30, 139-145 (2016)
DOI: 10.1016/j.tmrv.2016.03.001

8. X Wang, WC Chang, CW Wong, D Colcher, M Sherman, JR Ostberg, SJ Forman, SR Riddell, MC Jensen. A transgene-encoded cell surface polypeptide for selection, *in vivo* tracking, and ablation of engineered cells. *Blood* 118, 1255-1263 (2011)
DOI: 10.1182/blood-2011-02-337360

9. DT Rodgers, M Mazagova, EN Hampton, Y Cao, NS Ramadoss, IR Hardy, A Schulman, J Du, F Wang, O Singer, *et al.* Switch-mediated activation and retargeting of CAR-T cells for B-cell malignancies. *Proc Natl Acad Sci U S A* 113, E459-468 (2016)
DOI: 10.1073/pnas.1524155113

10. B Jena, B, S Maiti S, H Huls, H Singh, DA Lee, RE Champlin, LJ Cooper. Chimeric antigen receptor (CAR)-specific monoclonal antibody to detect CD19-specific T cells in clinical trials. *PLoS One* 8, e57838 (2013)
DOI: 10.1371/journal.pone.0057838

11. E Lanitis, M Poussin, IS Hagemann, G Coukos, R Sandaltzopoulos, N Scholler, DJ Powell, Jr. Redirected antitumor activity of primary human lymphocytes transduced with a fully human anti-mesothelin chimeric receptor. *Mol Ther* 20, 633-643 (2012)
DOI: 10.1038/mt.2011.256

12. E Lanitis, M Poussin, AW Klattenhoff, D Song, R Sandaltzopoulos, CH June, DJ Powell, Jr. Chimeric antigen receptor T Cells with dissociated signaling domains exhibit focused antitumor activity with reduced potential for toxicity *in vivo*. *Cancer Immunol Res* 1, 43-53 (2013)
DOI: 10.1158/2326-6066.CIR-13-0008

13. LR Rodino-Klapac, CL Montgomery, WG Bremer, KM Shontz, V Malik, N Davis, S Sprinkle, KJ Campbell, Z Sahenk, KR Clark, *et al.* Persistent expression of FLAG-tagged micro dystrophin in nonhuman primates following intramuscular and vascular delivery. *Mol Ther* 18, 109-117 (2010)
DOI: 10.1038/mt.2009.254

14. LB John, C Devaud C, CP Duong, CS Yong, PA Beavis, NM Haynes, MT Chow, MJ Smyth, MH Kershaw, PK Darcy. Anti-PD-1 antibody therapy potently enhances the eradication of established tumors by gene-modified T cells. *Clin Cancer Res* 19, 5636-5646 (2013)
DOI: 10.1158/1078-0432.CCR-13-0458

15. LB John, MH Kershaw, PK Darcy. Blockade of PD-1 immunosuppression boosts CAR T-cell therapy. *Oncoimmunology* 2, e26286 (2013)
DOI: 10.4161/onci.26286

16. B Kasenda, A Kuhnl, I Chau. Beginning of a novel frontier: T-cell-directed immune manipulation in lymphomas. *Expert Rev Hematol* 9, 123-135 (2016)
DOI: 10.1586/17474086.2016.1122513

17. CL Bonifant, HJ Jackson, RJ Brentjens, KJ Curran. Toxicity and management in CAR T-cell therapy. *Mol Ther Oncolytics* 3, 16011 (2016)
DOI: 10.1038/mto.2016.11

18. XJ Xu, YM Tang. Cytokine release syndrome in cancer immunotherapy with chimeric antigen receptor engineered T cells. *Cancer Lett* 343, 172-178 (2014)
DOI: 10.1016/j.canlet.2013.10.004

19. JM Patel, GA Dale, VF Vartabedian, P Dey, P Selvaraj. Cancer CARtography: charting out a new approach to cancer immunotherapy. *Immunotherapy* 6, 675-678 (2014)
DOI: 10.2217/imt.14.44

20. ML Davila, I Riviere, X Wang, S Bartido, J Park, K Curran, SS Chung, J Stefanski, O Borquez-Ojeda, M Olszewska, *et al.* Efficacy and toxicity management of 19-28z CAR T cell therapy in B cell acute lymphoblastic leukemia. *Sci Transl Med* 6, 224ra225 (2014)
DOI: 10.1126/scitranslmed.3008226

21. SA Grupp, M Kalos, D Barrett, R Aplenc, DL Porter, SR Rheingold, DT Teachey, A Chew, B Hauck, JF Wright, *et al.* Chimeric antigen receptor-modified T cells for acute lymphoid leukemia. *N Engl J Med* 368, 1509-1518 (2013)
DOI: 10.1056/NEJMoa1215134

22. X Zhou, A Di Stasi, MK Brenner. iCaspase 9 Suicide Gene System. *Methods Mol Biol* 1317, 87-105 (2015)
DOI: 10.1007/978-1-4939-2727-2_6

23. T Zhang, L Cao, J Xie, N Shi, Z Zhang, Z Luo, D Yue, Z Zhang, L Wang, W Han, *et al.* Efficiency of CD19 chimeric antigen receptor-modified T cells for treatment of B cell malignancies in phase I clinical trials: a meta-analysis. Oncotarget 32, 33961-71 (2015)

Abbreviations: CAR, Chimeric Antigen Receptor; scFv, Single Chain Variable Fragment, PBS, Phosphate-Buffered Saline

Key Words: Chimeric antigen receptor, immunotherapy, cancer, cytokine, cell

Send correspondence to: Vita Golubovskaya, Promab Biotechnologies, 2600 Hilltop Drive, Richmond, CA 94806, Tel: 510-974-0694, Fax: 510-740-3625, E-mail: vita.gol@promab.com